Structure and Stability of the Negative Hydrogen Molecular Ion

B. Jordon-Thaden,[1] H. Kreckel,[1,*] R. Golser,[2] D. Schwalm,[1,3] M. H. Berg,[1] H. Buhr,[3,1] H. Gnaser,[4] M. Grieser,[1] O. Heber,[3] M. Lange,[1] O. Novotný,[1,5] S. Novotny,[1] H. B. Pedersen,[1,†] A. Petrignani,[1,‡] R. Repnow,[1] H. Rubinstein,[3] D. Shafir,[3] A. Wolf,[1] and D. Zajfman[3]

[1]*Max-Planck-Institut für Kernphysik, 69117 Heidelberg, Germany*
[2]*Universität Wien, Fakultät für Physik–Isotopenforschung, 1090 Wien, Austria*
[3]*Department of Particle Physics, Weizmann Institute of Science, Rehovot 76100, Israel*
[4]*Department of Physics and Research Center OPTIMAS, University of Kaiserslautern, D-67663 Kaiserslautern, Germany*
[5]*Columbia Astrophysics Laboratory, 550 West 120th Street, New York, New York 10027, USA*

(Received 17 August 2011; published 3 November 2011)

We present the results of a Coulomb explosion experiment that allows for the imaging of the rovibrational wave function of the metastable H_2^- ion. Our measurements confirm the predicted large internuclear separation of 6 a.u., and they show that the ion decays by autodetachment rather than by spontaneous dissociation. Imaging of the resulting H_2 products reveals a large angular momentum of $J = 25 \pm 2$, quantifying the rotation that leads to the metastability of this most fundamental molecular anion.

DOI: 10.1103/PhysRevLett.107.193003 PACS numbers: 33.15.Dj, 79.77.+g

Almost 50 years ago Taylor and Harris [1] showed that the $^2\Sigma_u^+$ H_2^- complex is instable relative to autodetachment into the $H_2 + e^-$ continuum for internuclear distances of less than 3 a.u. More recent theoretical considerations [2,3] indicated extremely short lifetimes ($\sim$ 10–15 s), which would render a direct observation of H_2^- impossible. Experimentally, H_2^- ions are hard to identify as they have almost the same charge to mass ratio as the stable D^- ion. Nevertheless, mass spectroscopic detection of H_2^- was first described in 1957 by Khvostenko and Dukel'Skii [4], followed by reports in the 1970s of H_2^- creation in a duoplasmatron source [5] and observations of HD^- and D_2^- in ion beams at accelerator facilities [6]. However, when a careful—albeit unsuccessful—search for metastable negative hydrogen ions was carried out by Bae *et al.* in 1984, the authors concluded that "H_2^- (and H_3^-), do not, in fact, exist metastably" [7]. Since then, reported detections were traditionally met with skepticism based on the experimental difficulties and lack of reproducibility. This notion was corrected only recently by the definitive detection of H_2^-, D_2^-, and H_3^- at the VERA tandem accelerator [8], by ensuing lifetime measurements [9], and by a photofragment imaging experiment of D_2^- [10].

In reaction dynamics, the H_2^- complex has long been assumed to play a key role as a transient state in many fundamental reactions like dissociative attachment (DA: $e^- + H_2 \rightarrow H_2^- \rightarrow H + H^-$) and associative detachment (AD: $H + H^- \rightarrow H_2^- \rightarrow H_2 + e^-$), since the magnitude of the cross section for these processes suggests a resonant mechanism (see [3] and references therein). The latter process is the dominant formation mechanism of H_2 molecules in the epoch of first star formation in the early Universe [11]. The nonlocal theory that was employed to model the H_2^- collision complex in [3,11] has also been applied to explain long-lived H_2^- states [12] observed in the ion trap measurements. It predicts a shallow potential minimum formed by a centrifugal barrier at large internuclear distances that supports vibrational states with $v = 0$ for rotational angular momenta up to $J = 27$, which are metastable against autodetachment into $H_2 + e^-$ and fragmentation into $H^- + H$ [8,12].

To study the structure of metastable H_2^-, we have performed foil-induced Coulomb explosion imaging (CEI) measurements [13,14]. By triggering a Coulomb explosion on a time scale of 100 as [13], these measurements allow us to determine the square of the nuclear wave function of the molecule as a function of the internuclear distance R [15]. Negative ions with 2 atomic mass units were extracted from a cesium sputter source utilizing a solid HfH_2 target. The ion beam with a current of 500 pA was accelerated to 0.97 MeV by a linear radiofrequency quadrupole accelerator and magnetically guided into the CEI beam line (Fig. 1). The beam consisted mainly of D^- ions ($> 99.9\%$) with only a small fraction of H_2^-. Moreover, of the metastable H_2^- states produced in the source, only the longest-lived state, with a lifetime of 8.2 ± 1.5 μs [9,12], is expected to survive the flight time of $\sim$11 μs from the source to the CEI setup.

Behind the last bending magnet, the ion beam was collimated by two apertures of 1 and 1.5 mm diameter, respectively, before traversing an ultrathin diamondlike carbon (DLC) foil of $\sim$0.8 $\mu g/cm^2$. Upon entrance in the foil all electrons are stripped off instantaneously while the bare protons and deuterons traverse and exit the foil almost unperturbed. The D^+ ions were discriminated from the protons by a magnetic field separator behind the stripping region; thus only the two protons resulting from the Coulomb explosion of diatomic hydrogen were detected.

The time scale of electron stripping in the foil amounts to 10^{-16} s, which is much shorter than the time scales of

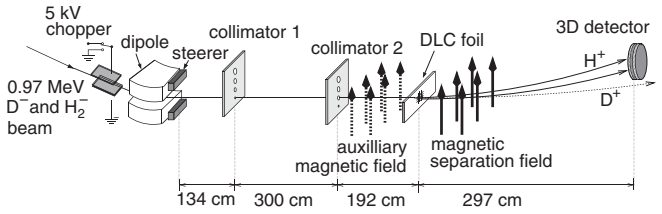

FIG. 1. Schematic of the CEI beam line (distances not to scale). After collimation the ions pass through a diamondlike carbon (DLC) foil that strips off all electrons. The stripping foil covers an aperture of 2 mm diameter in a stainless steel holder. A magnetic field guides the two protons from the Coulomb explosion of H_2^- towards a 3D imaging detector, while D^+ ions—resulting from electron stripping of D^-, the unwanted main constituent of the beam—are discriminated. An auxiliary magnetic field can be introduced before the DLC foil to deflect all charged particles prior to entering the stripping region.

molecular rotation (10^{-12} s) or vibration (10^{-14} s) and therefore the internuclear distance R can be considered frozen during the stripping process. Without the binding electrons, the two bare protons are driven away from one another by their mutual Coulomb repulsion and the potential energy $E_C \sim e^2/R$ is rapidly converted into kinetic energy [13]. The total energy release is determined by a three-dimensional (3D) imaging detector [14] located 3 m downstream of the stripping foil, where the protons have gained distances of a few centimeter. For 3D imaging, the detector records the spatial distance of the protons upon impact on a microchannel plate as well as their relative impact times for one molecule at a time. A fast high-voltage chopper before the last bending magnet prevents fragments from more than one molecule to reach the detector per event.

In a semiclassical description of the Coulomb explosion process (see Fig. 2) the kinetic energy distribution $P(E_{\mathrm{kin}})$ is related to the square of the nuclear wave function $\Psi_{\nu,J}(R)$ by [16]

$$P(E_{\mathrm{kin}}) \sim |\Psi_{\nu,J}(R)|^2 \left| \frac{dR}{dE_{\mathrm{kin}}} \right|. \tag{1}$$

The measured kinetic energy E_{kin} for an individual molecular event is connected to the internuclear distance R upon entrance into the foil by

$$E_{\mathrm{kin}}(R) = E_C(R) + \frac{\hbar^2}{2\mu R^2} J(J+1), \tag{2}$$

with μ denoting the reduced mass of H_2^-. We performed model calculations that showed that the semiclassical treatment results in a very good approximation of the fully quantum mechanical results.

The detailed Coulomb interaction, as well as small perturbations inside the foil, are incorporated in a Monte Carlo code of the Coulomb explosion process [17]. It computes classical trajectories, taking into account multiple scattering and charge exchange inside the foil [18], and the

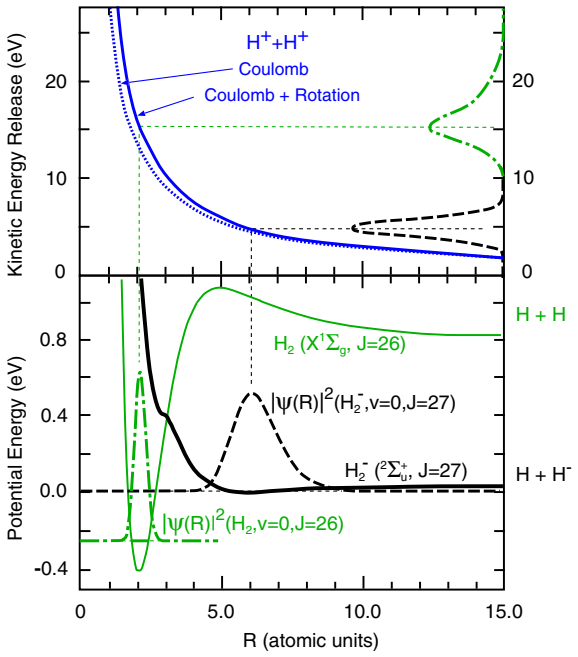

FIG. 2 (color online). Illustration of the Coulomb explosion principle for molecular hydrogen. Because of the fast stripping process the initial wave functions are projected vertically onto the Coulomb potential between the two bare protons. The measured kinetic energy release distributions are thus mirror images of the square of the initial wave functions, which are slightly shifted to higher energies due to the high angular momentum of the H_2^- ions. Shown in the lower panel are exemplary molecular potential curves for H_2^- and for the autodetachment product H_2 as well as the square $|\Psi(R)|^2$ of the nuclear wave functions corresponding to the $v = 0, J = 27$ state of H_2^- [20] and the $v = 0, J = 26$ state of H_2 [21]. The kinetic energy release as a function of the internuclear distance R and the resulting kinetic energy release distributions are displayed in the upper panel.

influence of the magnetic separation field and the detector efficiency. The momenta of the bound protons due to rotation are included in the simulation as initial velocities

$$v_J(R) = \frac{\hbar}{2\mu R}\sqrt{J(J+1)} \tag{3}$$

perpendicular to the molecular axis. (In principle the zero-point motion of the molecular vibration also adds to the initial velocity, but this contribution is negligible in the present case [16].) So-called "wake effects" arising from the interaction of the fast particles with the foil atoms [19] can be effectively eliminated by choosing only events that are near parallel to the detector plane. Therefore, all events with $\cos\alpha < 0.4$ (with α being the angle between the molecular axis and the detector plane) are discarded. The foil interactions are well understood and contribute around 20% to the width of the measured distribution.

Figure 3 displays the outcome of the CEI measurement (black dots) before cuts. The distribution shows a peak at a

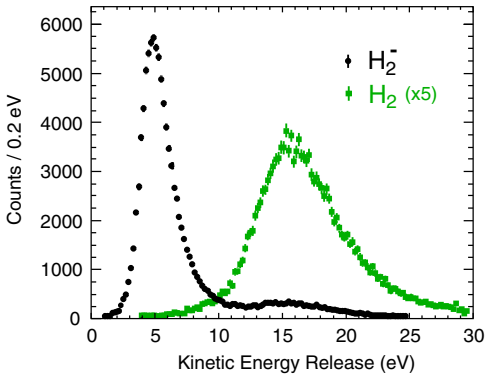

FIG. 3 (color online). Measured kinetic energy release after Coulomb explosion. The black dots show the distribution recorded with the H_2^- beam before cuts. The green squares show the KER distribution for the autodetachment product H_2, measured with the auxiliary magnetic field in front of the DLC target being switched on.

kinetic energy release of ~5 eV, attributed to H_2^-, and a second smaller peak around ~16 eV, which coincides with the kinetic energy release expected for neutral H_2 molecules. To verify whether the second peak is caused by neutral molecules, we introduced an auxiliary magnetic field between the second collimator and the stripping foil (see Fig. 1), thereby deflecting all charged particles before they enter the stripping region. In the distribution measured with this arrangement (green squares) the peak at 5 eV was absent while the 16 eV structure remained. Consequently, we assign the smaller peak to neutral H_2 molecules, created between the last bending magnet and the target foil.

By varying the pressure in the beam line, we found an upper limit of 10% for the fraction of the H_2 signal caused by stripping on residual gas. Hence the majority of the H_2 events stem from autodetachment. This finding is corroborated by tests with metastable D_2^- ions for which the sensitivity to residual gas induced D_2 events is much larger, as the relevant D_2^- states have considerably longer lifetimes against autodetachment [9,10,12]. Note that the experiment is not sensitive to the spontaneous dissociation of H_2^- into H and H^-. The two protons resulting from such an event behind the foil would hit the detector too closely together to be detected as two-body events.

From the relative intensities of the two peaks and the length of the straight section between steerer magnet and stripping foil, we can estimate the partial decay rate for autodetachment to be $2^{+1.3}_{-0.6} \times 10^5\ s^{-1}$. The largest contribution to the uncertainty is the influence of Earth's magnetic field, which leads to a slight difference in transmission between the H_2 and H_2^- ions through the beam collimators. The inverse of this autodetachment rate corresponds to a lifetime of $5 \pm 2\ \mu s$, which is shorter, but consistent within the error margins, with the previous lifetime measurement that yielded $8.2 \pm 1.5\ \mu s$ [9]. The present result thus reveals that autodetachment is indeed the dominant decay channel for the most long-lived H_2^- resonance.

The above-mentioned deflection of the H_2^- beam by the Earth's magnetic field leads to a small separation between the center-of-mass (c.m.s.) of the neutral H_2 events and the H_2^- events in the detector (xy) plane. By applying 1σ c.m.s. cuts in the respective x and y coordinates we can thus readily separate the H_2 and H_2^- events. The measured H_2^-

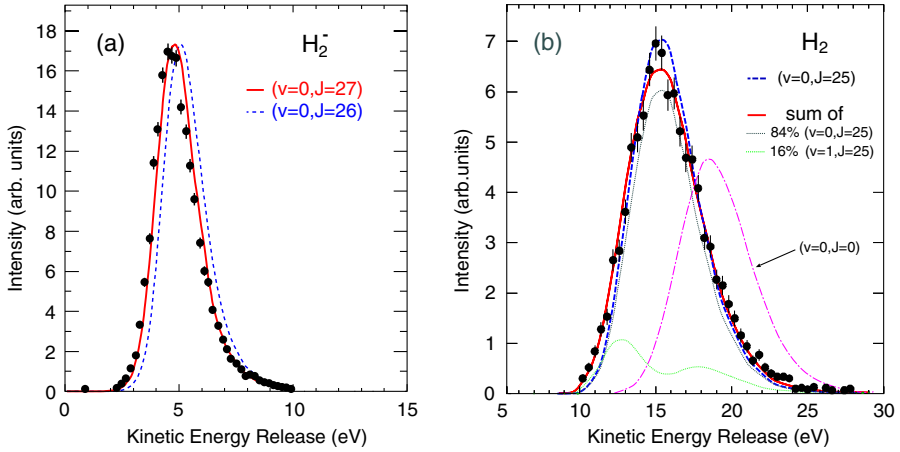

FIG. 4 (color online). Kinetic energy release (KER) distributions measured for (a) H_2^- and (b) H_2 after all cuts. The error bars reflect the statistical uncertainties on a 1σ level. The accuracy of the reconstructed kinetic energies is on the order of the symbol size. Also shown are fits with simulated distributions based on calculated wave functions. For H_2^- (a), the theoretical wave functions for the two longest-lived states are used [12,20]. Best agreement is found for the state with the maximum predicted lifetime of 6.3 μs (assigned with $v = 0$, $J = 27$) [12], while the distribution for the ($v = 0$, $J = 26$) state with the next-longest predicted lifetime of 0.38 μs is already clearly falling short of explaining the data. Note that the calculated H_2^- potential only supports states with $v = 0$ and $J \leq 27$ [12]. For the neutral autodetachment product H_2 (b), the KER distribution is best described by ($v = 0$, $J = 25$) when assuming only a single H_2 state to be populated (dashed blue curve). The agreement between simulation and data can be further improved by allowing also for a small $v = 1$ contribution (solid red curve).

KER distribution is plotted in Fig. 4(a). The distribution peaks at ~5 eV, directly revealing—independent of its detailed theoretical interpretation—that the average distance of the two protons in H_2^-, measured ~11 μs after its production, amounts to $\langle R \rangle \sim 6$ a.u. Moreover, the bell-shaped KER distribution readily identifies $v = 0$ as the dominant vibrational state. When comparing the measured KER distribution to simulated distributions based on theoretical H_2^- wave functions calculated by Čížek *et al.* [12,20], best agreement is found for the ($v = 0$, $J = 27$) state. This state is also predicted to have the longest lifetime of 6.3 μs [12], close to the measured lifetime of 8.2 ± 1.5 μs [9].

Direct experimental information on the rotational quantum number of the H_2^- state can be inferred from the analysis of the KER distribution of the H_2 decay product shown in Fig. 4(b). Using simulated distributions based on the well-known rovibrational H_2 wave functions [21], a χ^2 fit of the measured distribution, assuming only a single ($v = 0$) state to contribute, results in $J = 25$. Remaining differences between the measured and simulated distributions may be either due to a small contribution of a ($v = 1$) state, which are still energetically accessible in the decay of H_2^- for $J < 26$, or due to an additional broadening effect caused by the divergence of the H_2 beam, which is difficult to account for. Given the precision of the data and the quality of the fits, we conclude that our measurement confines the rotational quantum number of the autodetached H_2 molecules to $J = 25 \pm 2$.

As theoretical considerations suggest that autodetachment will be dominated by an outgoing p-wave ($\Delta J = \pm 1$) electron [22], with a strong preference for $\Delta J = -1$ for energetic reasons, this result supports the $J = 27$ assignment for the most long-lived H_2^- state.

In summary, we present experimental results for the structure and lifetime of the most fundamental molecular anion H_2^-. After decades of speculation, our measurements confirm the predicted mechanism lending metastability to the H_2^- complex not only on a qualitative level, but also quantitatively, and they provide a comprehensive verification of the theoretical description.

CEI measurements of the more long-lived D_2^- ion are presently being analzyed. Further motivation to study small negative ions comes through recent theoretical calculations that predict stable negative triatomic hydrogen ions [23] and the suggestion that H_3^- may be detectable in interstellar space [24]. Therefore it is foreseen to carry out Coulomb explosion measurements with H_3^- and D_3^- in the near future.

The authors thank M. Čížek for providing his calculated H_2^- wave functions. The authors also thank S. Altevogt, D. Bing, J. Hoffmann, and M. B. Mendes for technical assistance, L. Lammich for helpful discussions, and V. Kh. Lichtenstein for providing the DLC foils. This research was supported by the German-Israeli Foundation for Scientific Research and Development (G.I.F.) under Grant No. I-900-231.7/2005. D. Sch. acknowledges support by the Weizman Institute through the Joseph Meyerhoff program. H. B. was supported by the European Project ITS LEIF (HRPI-CT-2005-026015).

*hkreckel@illinois.edu
Present address: Chemistry Department, University of Illinois, 61801 Urbana, IL, USA.
†Present address: Department of Physics and Astronomy, University of Aarhus, DK-8000 Aarhus, Denmark.
‡Present address: Leiden Observatory, Leiden University, PO Box 9513, NL-2300 RA Leiden, The Netherlands.

[1] H. S. Taylor and F. E. Harris, J. Chem. Phys. **39**, 1012 (1963).
[2] P. L. Gertitschke and W. Domcke, Phys. Rev. A **47**, 1031 (1993).
[3] M. Čížek, J. Horácek, and W. Domcke, J. Phys. B **31**, 2571 (1998).
[4] V. I. Khvostenko and V. M. Dukel'Skii, Sov. Phys. JETP **7**, 709 (1958).
[5] R. Hurley, Nucl. Instrum. Methods **118**, 307 (1974).
[6] W. Aberth, R. Schnitzer, and M. Anbar, Phys. Rev. Lett. **34**, 1600 (1975).
[7] Y. K. Bae, M. J. Coggiola, and J. R. Peterson, Phys. Rev. A **29**, 2888 (1984).
[8] R. Golser *et al.*, Phys. Rev. Lett. **94**, 223003 (2005).
[9] O. Heber *et al.*, Phys. Rev. A **73**, 060501 (2006).
[10] L. Lammich *et al.*, Phys. Rev. A **80**, 023413 (2009).
[11] H. Kreckel *et al.*, Science **329**, 69 (2010).
[12] M. Čížek, J. Horáček, and W. Domcke, Phys. Rev. A **75**, 012507 (2007).
[13] Z. Vager, R. Naaman, and E. P. Kanter, Science **244**, 426 (1989).
[14] R. Wester *et al.*, Nucl. Instrum. Methods Phys. Res., Sect. A **413**, 379 (1998).
[15] Z. Amitay *et al.*, Science **281**, 75 (1998).
[16] Z. Amitay *et al.*, Phys. Rev. A **60**, 3769 (1999).
[17] D. Zajfman *et al.*, Phys. Rev. A **46**, 194 (1992).
[18] D. Zajfman *et al.*, Phys. Rev. A **41**, 2482 (1990).
[19] R. Garcia-Molina *et al.*, Nucl. Instrum. Methods Phys. Res., Sect. B **230**, 41 (2005).
[20] M. Čížek (private communication). The wave functions were calculated using an adapted molecular potential, which was introduced in Ref. [12] to better account for the lifetime measured for the most long-lived H_2^- state.
[21] R. J. Le Roy, LEVEL 8.0, University of Waterloo Chemical Physics Research Report No. CP-663, 2007; see http://leroy.uwaterloo.ca/programs/.
[22] M. Berman, C. Mündel, and W. Domcke, Phys. Rev. A **31**, 641 (1985).
[23] M. Ayouz *et al.*, J. Chem. Phys. **132**, 194309 (2010).
[24] M. Ayouz *et al.*, Phys. Rev. A **83**, 052712 (2011).